

Xu Yang\*,  
Zhang Ziyu,  
Li Angang,  
Sheng Xiaowei

# Noise Source Identification Method for a Warp Machine Based on MEEMD\_AIC

DOI: 10.5604/01.3001.0013.9019

Donghua University Shanghai,  
School of Mechanical Engineering,  
Shanghai, China,  
\* e-mail: xuyang@dhu.edu.cn

## Abstract

*In order to recognise the noise source of a warp knitting machine, a method based on Modified Ensemble Empirical Mode Decomposition (MEEMD) and Akaike Information Criterion (AIC) is proposed. The MEEMD\_AIC method is applied to measure the noise signal of a warp knitting machine and analyse every single effective component selected. Noise source identification is realised by combining the vibration signal characteristics of the main parts of the warp knitting machine. Firstly, MEEMD is used to decompose the measured noise signal of the warp knitting machine into a finite number of intrinsic mode function (IMF) components. Then, singular value decomposition (SVD) is performed on the covariance matrix of the component matrix to get the eigen value of the matrix. Next, the number of effective components is estimated based on the AIC criterion, and the effective components are selected by combining the energy characteristic index and the Pearson correlation coefficient method. The results show that the noise signal of the warp knitting machine is a mixture of multiple noise source signals. The main noise sources of the warp knitting machine, including the vibration of the pulling roller, the main shaft of the loop forming mechanism and the push rod of the guide bar traverse the mechanism, provide theoretical support for recognition of the active noise reduction of the warp knitting machine using the MEEMD\_AIC method.*

**Key words:** warp machine, noise source identification, modified ensemble empirical mode decomposition, Akaike Information Criterion.

pact, friction and other conditions often with more than one noise source. Even the same sound source often has multiple parts that produce sound, and the noise condition is unusual and complex. Therefore, it is necessary to clearly grasp the characteristics of each sound source and the weight of its total noise, as well as to locate and identify the main sound sources in order to formulate reasonable noise reduction measures for a warp knitting machine with multiple noise sources.

The problem of Blind Source Separation (BSS) [3] is to separate and identify the noise source signal from the observation signal, which is obtained by mixing the unknown source signal, which mainly includes two parts: source number estimation and source separation. Because of the complexity of the warp knitting machine structure and the numerous noise sources, the first step is to estimate the number of sources before source identification under the condition of limited experimental conditions; however, the number of noise sources cannot be determined directly in the actual test process. Empirical Mode Decomposition (EMD), which was proposed by Huang E [4] et al, is a blind signal processing method to stabilise non-linear non-stationary signals. Modified Ensemble Empirical Mode Decomposition (MEEMD), which was proposed by Lian C [5], is an improved algorithm of EMD, which can solve the modal aliasing problem of EMD and the modal splitting problem of

Ensemble EMD (EEMD) [6]. At present, EMD and its improved algorithm have been widely used in many fields, such as fault diagnosis [7-8], weather prediction [9-10], medical and health care [11], etc.

In this paper, the MEEMD algorithm is combined with the Akaike Information Criterion (AIC) source number estimation method and MEEMD\_AIC method for the noise source identification of warp knitting machines. Then the MEEMD\_AIC method is applied for identification of the noise source of a warp knitting machine, and its main noise source is accurately identified, which provides theoretical support for the active noise reduction of the warp knitting machine.

## Noise characteristic analysis of a warp knitting machine

### Structure of the warp knitting machine

In this paper, the experiment object is a 3.5 m double needle bed warp knitting machine, produced by the Karl Mayer Company of Germany, which is shown in **Figure 1**. The components of this machine are shown in **Figure 2**. The warp knitting machine is mainly composed of four parts: the let-off mechanism, the loop forming mechanism, the guide bar traverse mechanism, the pulling and coiling mechanism, the driving mechanism and the auxiliary device. Among them, the let-off mechanism is mainly used to send the warp yarn to the loop form-

## Introduction

OSHA [1] stipulates that for single level noise, continuous noise exposure shall not exceed 90 dB when working for more than 8 hours. In 2013, China's newly revised GB/T 50087-2013 "Code for the Design of Noise Control of Industrial Enterprises" [2] stipulates that the noise floor of the workshop is 85 dB, which is 5 dB lower than OSHA. Even with improvement of the characteristics of the warp knitting machine, such as making it wide, heavy, high-speed and complex in the mechanism, the noise generated is greater. Therefore, research on the noise reduction of textile machinery is urgent and of great significance.

Generally speaking, the structure of the warp knitting machine is as complex as its transmission path. In the weaving process, there is high-speed rotation, reciprocating, multi-motion coupling, im-

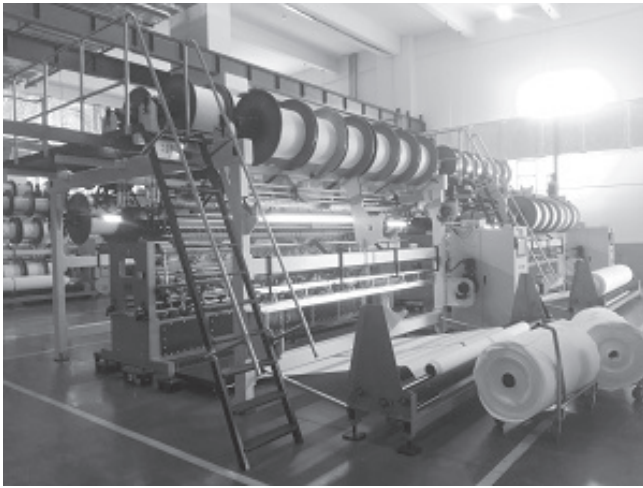


**Figure 1.** Structure of warp knitting machine.

The main function of the transmission mechanism is to coordinate the work of each part and complete the warp knitting process, while the auxiliary mechanism is mainly used to realise intelligent production on the warp knitting machine.

Under the operating condition that the main shaft speed of the warp knitting machine is 300 rpm, LV-FS01 and Quick Signal Analyzer (Quick SA) real-time signal analysis software are used to collect the vibration signals of the main vibration parts of the warp knitting machine, and the collected vibration signals are analysed one by one. The main vibration frequencies of the parts are shown in **Table 1**. The sampling frequency is set to 8192Hz and the sampling time is 4 s.

**The acquisition and preprocessing of noise signals**

Under the same conditions, the noise signals of the warp knitting machine near the workers' ears are collected. According to GB/T 7111.6-2002 "Textile machinery – Noise test code Part 6: Fabric manufacturing machinery", the sound pressure sensor is arranged at a distance of 1 m from the machine surface, and at a height of 1.6 m from the table position.

**Table 1.** Main vibration frequency of the warp knitting machine parts.

Part	Main vibration frequency, Hz
Main motor	35.45
Pulling motor	60.437
Guide bar	15.45
Sinker	5
Guide bar moving putter	35.45
Yarn guide rod	15
Lever 1	5
Lever 2	15
Lever 3	5
Machine base	5.15.45

ing mechanism with a certain amount of let-off for knitting; the loop forming mechanism is used to complete the loop forming movement of the warp knitting machine; the main function of the guide needle on the guide bar is to control the traverse movement before and after the warp knitting machine, and assist the loop forming mechanism in completing the fabric weaving; and the pull and take-up mechanism carries out loop forming The coil is pulled away from the knitting area at a certain speed and wound on the winding shaft with a certain tension.

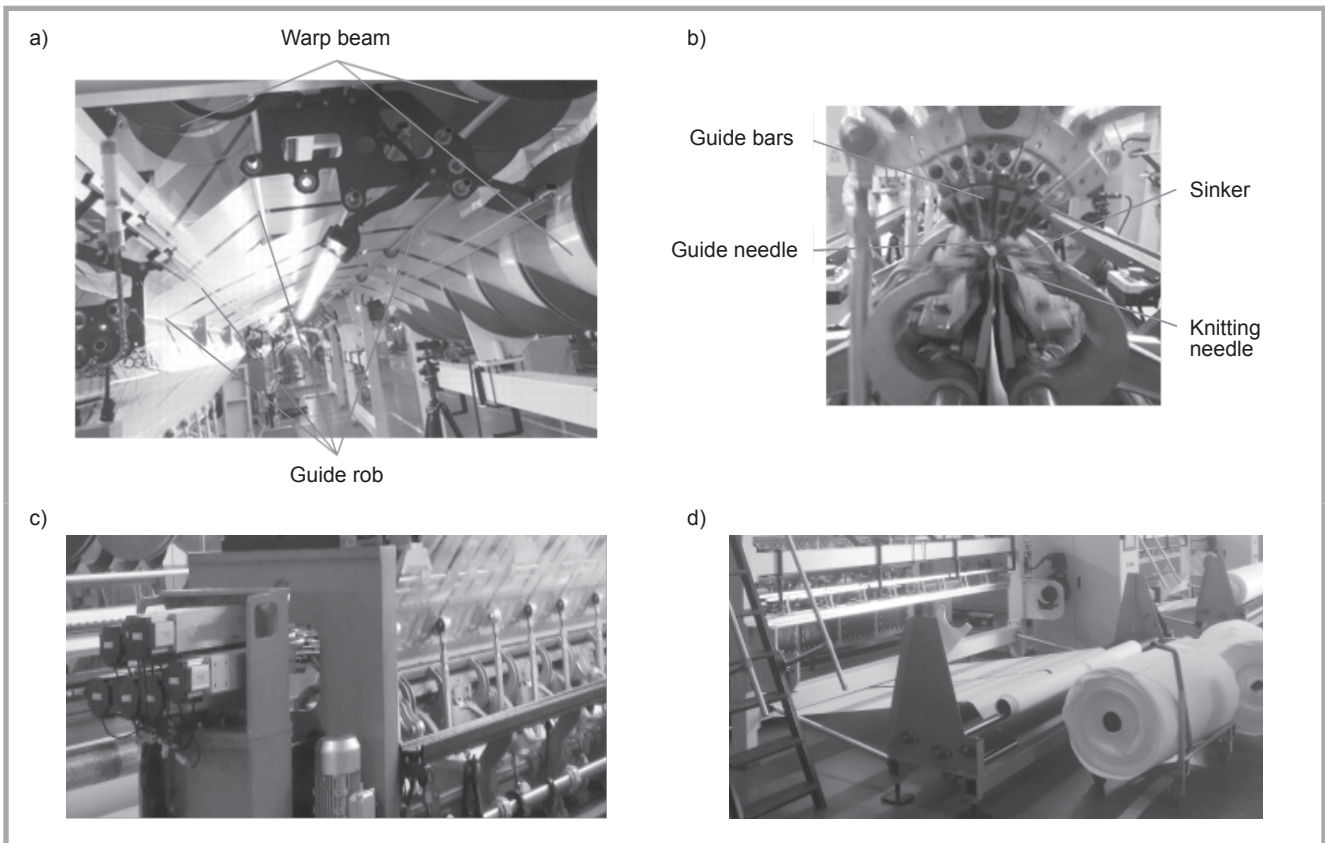


**Figure 2.** Schematic diagram of each composition of the warp knitting machine: a) warp let-off mechanism, b) loop forming mechanism, c) guide bar traverse mechanism, d) pulling and coiling mechanism.

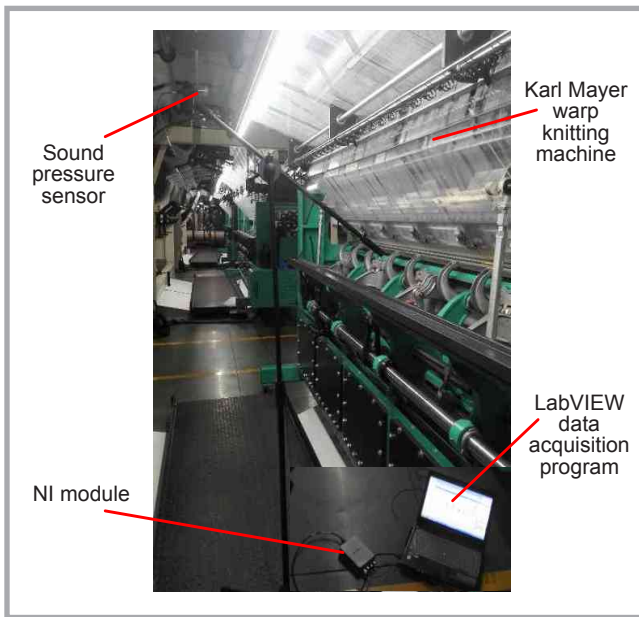


**Figure 3.** Experimental arrangement.

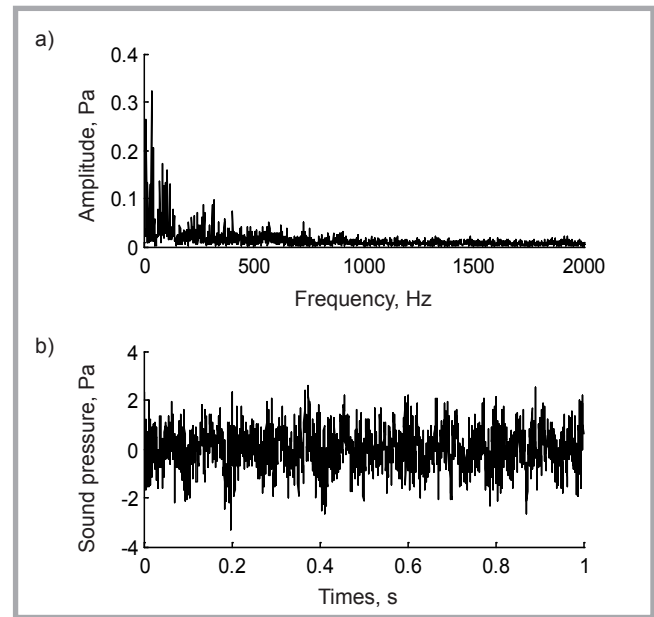


**Figure 4.** Figures for the pretreatment of the noise signal: a) waveforms of the signal, b) spectrum of the signal.

The noise signals are collected in this experiment by a sound pressure sensor-BK4961, combined with an NI-9234 C Series sound and vibration input module and corresponding LabVIEW data acquisition program. The sampling frequency is 8192 Hz and the sampling time 8 s. A total of 6 experiments are carried out, and the experimental site layout is shown in **Figure 3**.

All the noise signals collected are analysed preliminarily. In order to improve the computational efficiency, a typical data length of 1 s is selected as the analysis object. The signal waveform and spectrum obtained after the fast Fourier transform of the signal are shown in **Figure 4**.

In the working condition where the spindle of the warp knitting rotates at a speed of 300 r/min, the movement frequency of the impact and friction between various parts of the knitting elements is 5 Hz. However, the fact that the impulse noise in the noise signal is covered by the background noise leads to the result that the impact characteristics of the 5 Hz signal cannot be identified through the noise signal waveform shown in **Figure 4.a**. **Figure 4.b** is the amplitude and frequency of the noise signal. It is seen in the figure that the frequency of the noise signals is mainly distributed below 400 Hz. And the frequency component is complex, mainly composed of low-frequency noise within 0-100 Hz.

An appropriate window function is used for short-time Fourier transform of the noise signal near the workers' ears. It is clear from the time-frequency diagram shown in **Figure 5** that the noise source is not unique. The signal characteristics of each frequency band are shown in **Table 2**.

### MEEMD\_AIC noise recognition algorithm

The heart of the MEEMD\_AIC approach is the MEEMD algorithm and AIC guide-

lines. From the MEEMD\_AIC algorithm flow chart shown in **Figure 6**, the specific steps are as follows:

- 1) **MEEMD decomposition of the signal.** MEEMD decomposition of the single-channel observation signal yields a finite number of IMF components.
- a) Add two sets of positive and negative white noise signals of equal absolute value to the signal to be decomposed so that the time scale of the signal is continuous and then do EEMD de-

**Table 2.** Signal characteristics of each frequency band.

Frequency band	Signal characteristics
400-600 Hz	Showing a certain periodicity, and with the spindle rotation cycle
200-300 Hz	Periodicity is not obvious, but 5 Hz time-frequency changes can still be distinguish
100 Hz or so	Signal did not change significantly over time, time-invariant stable signal
0-50 Hz	Signal did not change significantly over time, time-invariant stable signal

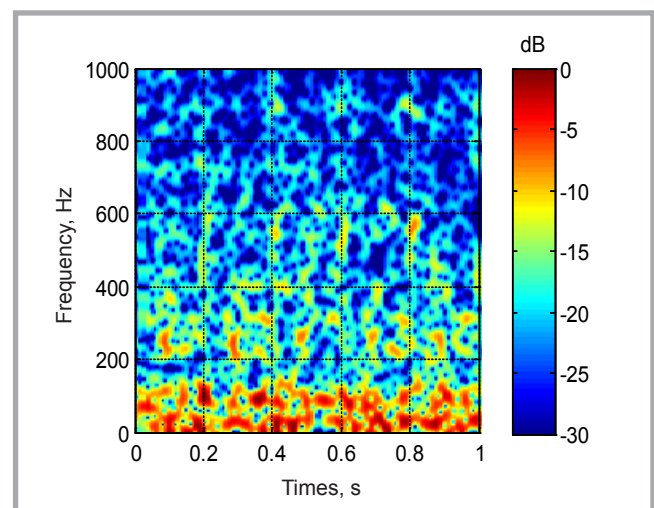


**Figure 5.** Time-frequency of the signal.

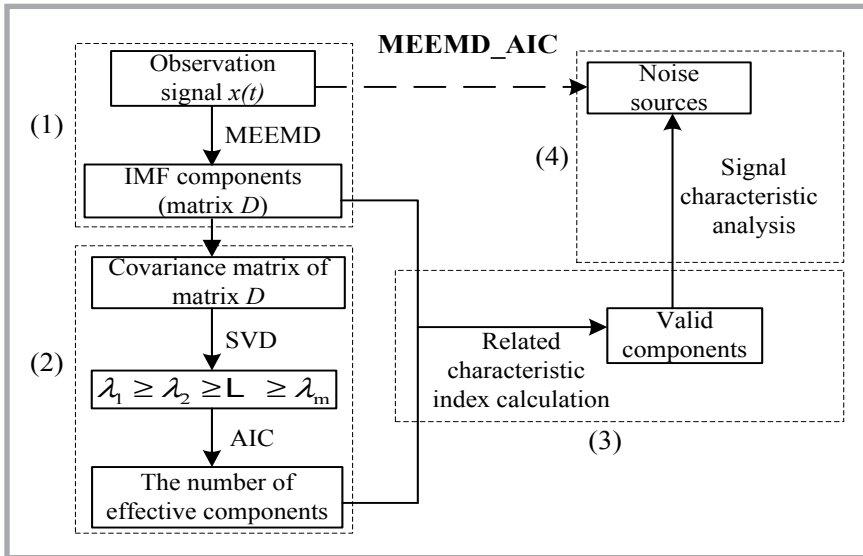


Figure 6. Flow chart of MEEMD\_AIC algorithm.

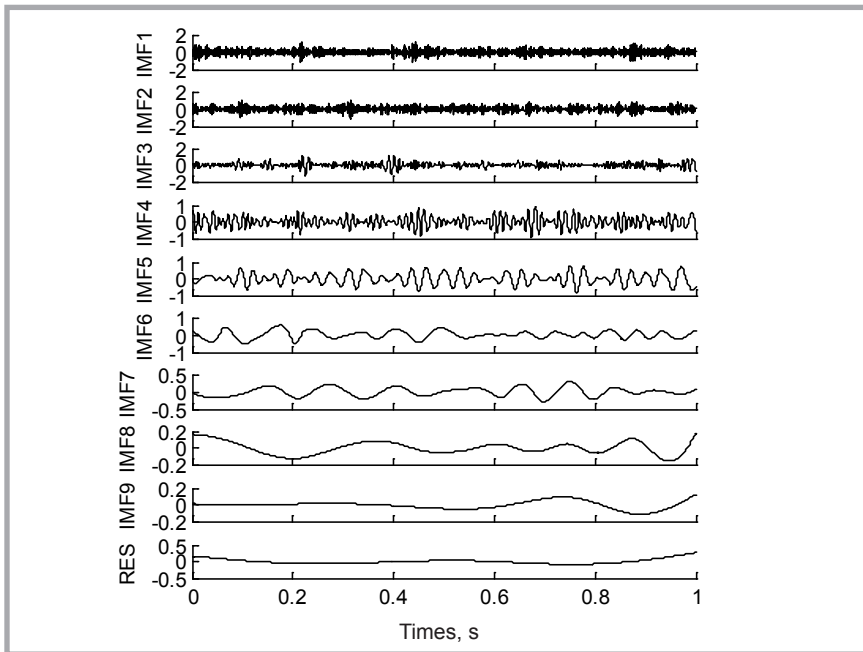


Figure 7. Results of MEEMD decomposition.

- composition with the same number of aggregate average on the two groups of signals;
- b) The residual white noise can be eliminated to the greatest extent by averaging the corresponding components of the two groups of decomposition results in a);
  - c) Since the result of the aggregate average is not necessarily the standard IMF component, EMD decomposition is needed for this group of components; Finally, MEEMD can be expressed as:

$$x(t) \xrightarrow{\text{MEEMD}} \sum_{l=1}^m [d_l(t)] + r(t) \quad (1)$$

The  $d_l(t)$  in Eq. (6) represents the IMF component obtained finally,  $l = 1, 2, \dots, m$ , and  $r(t)$  represents the final residual component.

### 2) Estimate of the number of effective components.

- a) After the signal is decomposed by MEEMD, the IMF component matrix is obtained. By SVD decomposition of the covariance matrix of the matrix, multiple eigenvalues corresponding to IMF components can be obtained.
- b) Due to the noise background of the warp knitting machine being coloured noise, the accuracy of the AIC criterion for estimating the number of sourc-

es in the background of coloured noise is poor. For this reason, Rui Chen [12] smoothed out the noise eigenvalues by diagonally loading the covariance matrix so that the improved method can be applied to the background of coloured noise. The corrected eigenvalue  $\mu_i = \lambda_i + \lambda_{DL}$ ,  $i = 1, 2, \dots, m$ , where the loading  $\lambda_{DL} = \sqrt{\sum_{i=1}^m \lambda_i}$ . After eigenvalue correction:

$$AIC(k) = -2N(m-k) \lg \left( \frac{\prod_{i=k+1}^m \mu_i}{m-k} \right) + 2k(2m-k) \quad (2)$$

Where,  $N$  is the number of samples, and  $k = 1, 2, \dots, m-1$ . Calculate the AIC value of  $k$  from 1 to  $m-1$ . The  $k$  corresponding to the smallest AIC value is the number  $n$  of effective components.

Combining the energy characteristic index with the Pearson correlation coefficient method [2], the total energy of each IMF and the correlation coefficient between the IMFs and the original signal are calculated, separately, and all the IMF components obtained after signal decomposition are reordered to find the most significant components  $n$  of the relevant feature index.

### 3) Screening effective components.

Combining the energy characteristic index with the Pearson correlation coefficient method [2], the total energy of each IMF and the correlation coefficient between the IMFs and the original signal are calculated separately, and all the IMF components obtained after signal decomposition are reordered to find the most significant components  $n$  of the relevant feature index.

- 4) **Noise source identification.** In turn, the effective components  $n$  are analysed for signal characteristics to complete the noise source identification.

## Noise source identification of warp knitting machine

### MEEMD Decomposition of Noise Signal of Warp Knitting Machine

MEEMD decomposition of the noise signal was done. The white noise amplitude was added to 0.2 times the rms value of the noise signal, and the lumped average

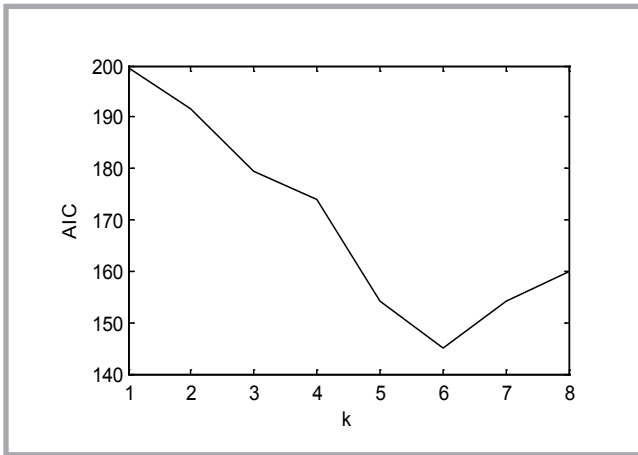


Figure 8. Calculation results of AIC.

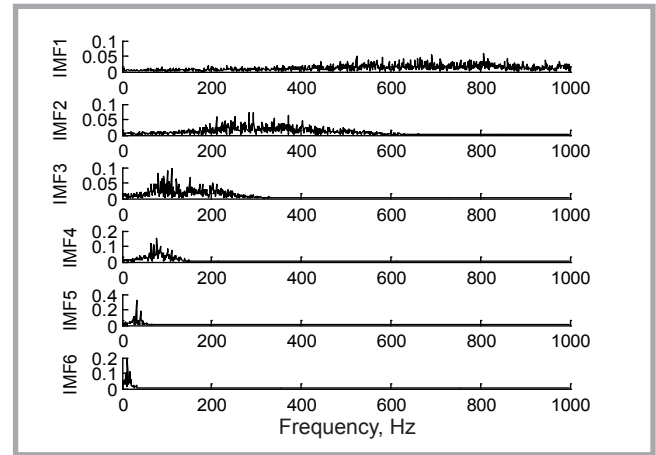


Figure 9. Amplitude-frequency diagram of effective components Time-frequency diagrams of components IMF3 and IMF4 are shown in Figure 10.

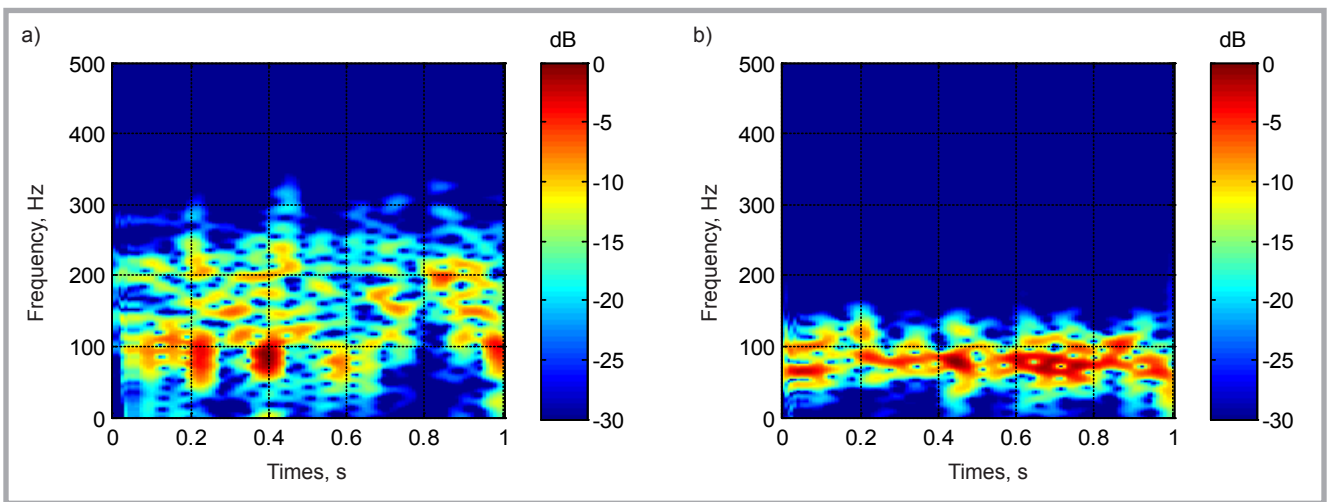


Figure 10. Time-frequency of IMF3 and IMF4: a) IMF3, b) IMF4.

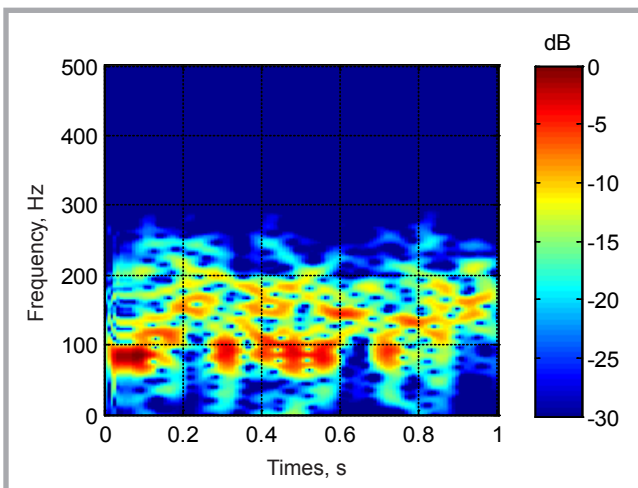


Figure 11. Time-frequency of IMF3 of the background noise.

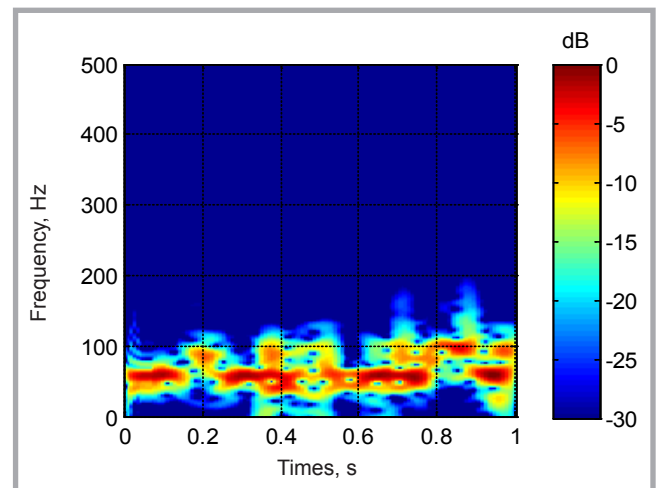


Figure 12. Time-frequency of IMF3 of the pulling motor.

Table 3. Calculation results of all IMF components.

Component	IMF1	IMF2	IMF3	IMF4	IMF5	IMF6	IMF7	IMF8	IMF9
Total energy/Pa <sup>2</sup>	241.940	168.338	205.023	167.530	212.304	112.240	29.103	11.653	3.127
Correlation coefficient	0.455	0.406	0.422	0.414	0.400	0.315	0.165	0.044	0.026

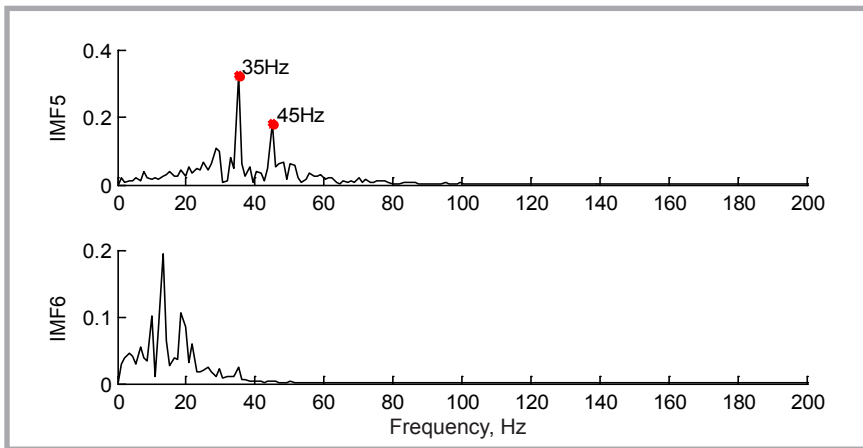


Figure 13. Amplitude-frequency of IMF5 and IMF6.

was 200 times. 9 IMF components were obtained. The decomposition result is shown in Figure 7.

#### Estimation of effective component number of warp knitting machine noise

The covariance matrix of the IMF component matrix is calculated and SVD decomposed. The following eigenvalues were obtained: 0.1215, 0.1103, 0.1017, 0.0838, 0.0809, 0.0559, 0.0144, 0.0057, 0.0016. The AIC value after eigenvalue correction is shown in Figure 8. The estimated number of valid components is 6 as the smallest AIC value corresponds to  $k = 6$ .

#### Screening of effective components of warp knitting machine noise

Combining the evaluation index of energy characteristics and Pearson's correlation coefficient method, the total energy and correlation coefficient of each IMF with the original signal are calculated, respectively. The calculation results are shown in Table 3. It can be seen from Table 3 that the total energy and correlation coefficients of the IMF1 ~ IMF6 components are large. As the number of effective components of the warp knitting machine decomposed by MEEMD is 6, components IMF1 ~ IMF6 are effective. Components IMF7 ~ IMF9 are false as their total energy and correlation coefficient are small.

#### Characteristic analysis of effective noise components and noise source identification

Each amplitude-frequency figure of each effective component of warp knitting machine noise shown in Figure 9 is obtained through the Fast Fourier trans-

form. Comparing the amplitude-frequency figures, it can be seen that the IMF1 and IMF2 components have a wider frequency distribution but a smaller amplitude, being similar to the components obtained after MEEMD decomposition of Gaussian white noise. Therefore, it can be determined that components IMF1 and IMF2 are background noise without noise source units.

Background noise signals in the factory are collected and decomposed by MEEMD. Component IMF3 of the decomposition results is shown in Figure 11. Comparing Figure 11 with Figure 10.a, it can be found that the frequency distribution of the two components is similar and that all signal frequency characteristics change with time. Therefore, it can be judged that component IMF3 of the warp knitting machine noise is also derived from the background noise.

It is known from Table 1 that there is more than one excitation source of the pulling motor vibration signal. Decomposing the signal through MEEMD, the time-frequency diagram of IMF3 is obtained, shown in Figure 12. Comparing Figure 12 with Figure 10.b, it can be found that their time-frequency characteristics are consistent. The pulling roller controlled by the pulling motor is long, leading to an obvious vibration. As a result, component IMF4 of the warp knitting machine noise signal comes from the vibration of the pulling roller.

Because of the fact that the signals of IMF5 and IMF6 from Figure 7 are not obvious with time, they can be regarded as time invariant signals. The amplitude-frequency images of IMF5 and IMF6 are extracted from Figure 9 and

amplified in the frequency axis, resulting in Figure 13. It is shown in Figure 13 that the main frequencies of component IMF5 are 35 Hz and 45 Hz. It can be seen from Table 1 that the main vibration frequency of the main motor and guide bar moving putter are both 35 and 45 Hz. It is known that the motor of the guide bar moving elements and the main motor are mounted on the same side of the warp knitting machine rack. The vibration intensity is greater because their vibrations can pass to each other. Hence, the noise shown by component IMF5 is the sum of the vibration noise of the spindle in the looping mechanism and the guide bar moving putter.

The frequency of the IMF6 component in Figure 13 is mainly distributed below 20 Hz. The audible frequency range of the human ear is from 20 Hz to 20 kHz. The noise shown by the component is out of the range, and hence it is not needed for noise source identification.

## Conclusions

In this paper, using the MEEMD\_AIC algorithm combined with the warp knitting machine structure characteristics and related experimental analysis, the noise sources of the warp knitting machine are identified, concluded as follows:

- 1) This paper presents a MEEMD\_AIC algorithm which is suitable for the noise source identification of warp knitting machines. Experiments show that the algorithm can accurately identify the effective components from a single-channel noise signal, and it is suitable for the analysis of the noise signal of warp knitting machines.
- 2) The MEEMD\_AIC algorithm is used to deal with noise measured near the ear of the warp knitting machine worker. Six effective components of the noise of the warp knitting machine are obtained, among which the first three are noise components coming from the background noise.
- 3) Based on the analysis of the remaining 3 effective components, combined with the vibration characteristics of each machine part of the warp knitting machine, it is concluded that the noise near the ear of the warp knitting machine worker is mainly composed of the vibration noise of the pulling roller, the spindle in the looping mechanism and the guide bar moving putter.

## References

1. 1910 OSHA Guide. Occupational Health and Environmental Control[S]. 2014. Occupational Health and Environmental Control, 1910, 95[S].
2. Ministry of Housing and Urban-Rural Development of the People's Republic of China. GB/T 50087-2013, Code for Design of Noise Control of Industrial Enterprises[S]. Beijing: China Building Industry Press, 2014. (in Chinese)
3. Wei Cheng, Zhengzheng Jia, Xuefeng Chen, Lin Gao. Convolutional Blind Source Separation in Frequency Domain with Kurtosis Maximization by Modified Conjugate Gradient[J]. *Mechanical Systems and Signal Processing* 2019, 134.
4. Huang N E, Shen Z, Long S R, et al. The empirical mode decomposition and the Hilbert spectrum for nonlinear and non-stationary time series analysis[J]. *Proceeding of the Royal Society of London Series a-Mathematical Physical and Engineering Sciences* 1998; 454A: 903-995.
5. Lian C, Zeng Z, Yao W, et al. Displacement Prediction Model of Landslide Based on a Modified Ensemble Empirical Mode Decomposition and Extreme Learning Machine[J]. *Natural Hazards* 2013; 66(2): 759-771.
6. Wu Z, Huang NE. Ensemble Empirical Mode Decomposition: A Noise-Assisted Data Analysis Method[J]. *Advances in Adaptive Data Analysis* 2009; 1 (1): 1-41.
7. Guo T, Deng Z M. An Improved EMD Method Based on the Multi-Objective Optimization and Its Application to Fault Feature Extraction of Rolling Bearing[J]. *Applied Acoustics* 2017; 127: 46-62.
8. Yu K, Lin T R, Tan JW. A Bearing Fault Diagnosis Technique Based on Singular Values of EEMD Spatial Condition Matrix and Gath-Geva Clustering[J]. *Applied Acoustics* 2017; 121: 33-45.
9. Wang WC, Chau KW, Qiu L, et al. Improving Forecasting Accuracy of Medium and Long-Term Runoff Using Artificial Neural Network Based on EEMD Decomposition[J]. *Environmental Research* 2015; 139: 46-54.
10. Wang C, Zhang HL, Fan WH, et al. A New Chaotic Time Series Hybrid Prediction Method of Wind Power Based on EEMD-SE and Full-Parameters Continued Fraction[J]. *Energy* 2017; 138: 977-990.
11. Marcelo A C, Gastón S, María E T. Improved Complete Ensemble EMD: A Suitable Tool for Biomedical Signal Processing[J]. *Biomedical Signal Processing and Control* 2014; 14: 19-29.
12. Rui Chen, Fei Zhao, Changshui Yang, Yuan Li, Tiejun Huang. Robust Estimation for Image Noise Based on Eigenvalue Distributions of Large Sample Covariance Matrices[J]. *Journal of Visual Communication and Image Representation* 2019; 63.

☐ Received 29.08.2018      Reviewed 20.11.2019



**fiber fusion**  
MOTIVATE INNOVATE COLLABORATE

2020 MoFA KAWS Conference

- Leading Edge Textile Artists as Speakers and Teachers
- Classes, Workshops in all manner of fiber work
- May 2-4, 2020
- At beautiful Lake Doniphan in Excelsior Springs, Missouri (40 Minutes north of Kansas City)
- Pre-Conference Workshops April 30-May 1

<http://missourifiberartists.org>    <http://kcweaversguild.org>    Kansas Assoc. of Weavers & Spinners

**SAVE THE DATE**  
and be inspired.....



**ECOSUMMIT BERLIN**  
Smart green energy, mobility and cities  
6-7 May 2020 @ Radialsystem



International Conference and Exhibition on  
**Polymer Science and Technology**  
May 18-19, 2020 | Athens, Greece

Theme:  
Expedite Polymer Innovations for Solving Societal Challenges



**36TH INTERNATIONAL CONFERENCE OF THE POLYMER PROCESSING SOCIETY**  
MAY 31 - JUNE 4, 2020  
LE CENTRE SHERATON, MONTREAL (QC), CANADA